AD-A174 620 ELECTROMAGNETIC SENSOR ARRAYS FOR NONDESTRUCTIVE EVALUATION AND ROBOT CON (U) STANFORD UNIV CA EDWARD L GINZTON LAB OF PHYSICS B A AULD ET AL OCT 86 1/1

UNCLASSIFIED AFOSR-TR-86-1073 F49620-84-C-0095 F/G 17/6 NL

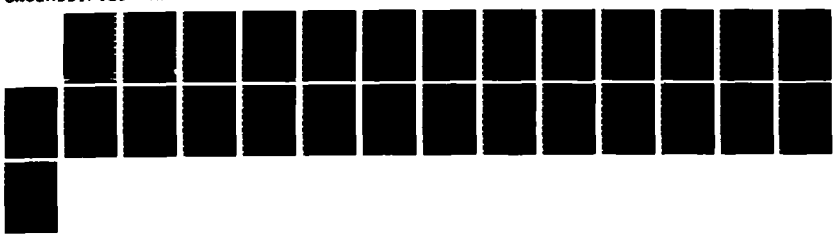

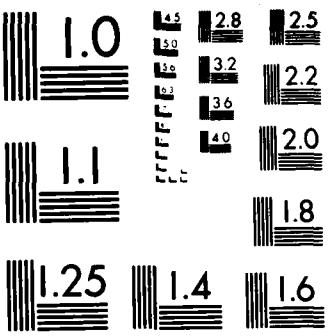

MICROCOPY RESOLUTION TEST CHART
NATIONAL BUREAU OF STANDARDS-1963-A

UNCLASSIFIED

AD-A174 620

REPORT DOCUMENTATION PAGE

1a. REPORT SECURITY CLASSIFICATION: UNCLASSIFIED	1b. RESTRICTIVE MARKINGS
2a. SECURITY CLASSIFICATION AUTHORITY	3. DISTRIBUTION/AVAILABILITY OF REPORT: Distribution is Unlimited
2b. DECLASSIFICATION/DOWNGRADING SCHEDULE	
4. PERFORMING ORGANIZATION REPORT NUMBER(S)	5. MONITORING ORGANIZATION REPORT NUMBER(S): AFOSR-TR- 86-1073
6a. NAME OF PERFORMING ORGANIZATION: Stanford University; 6b. OFFICE SYMBOL (If applicable)	7a. NAME OF MONITORING ORGANIZATION: Air Force Office of Scientific Research
6c. ADDRESS (City, State and ZIP Code): Edward L. Ginzton Laboratory, Stanford, Ca. 94305	7b. ADDRESS (City, State and ZIP Code): Bolling AFB, DC 20332-6448
8a. NAME OF FUNDING/SPONSORING ORGANIZATION: AFOSR; 8b. OFFICE SYMBOL (If applicable): NE	9. PROCUREMENT INSTRUMENT IDENTIFICATION NUMBER: F49620-84-C-0095
8c. ADDRESS (City, State and ZIP Code): Bld 410, B.A.F.B DC 20332-6448	10. SOURCE OF FUNDING NOS. — PROGRAM ELEMENT NO.: 61102F; PROJECT NO.: 2306; TASK NO.: A2; WORK UNIT NO.:
11. TITLE (Include Security Classification): ELECTROMAGNETIC SENSOR ARRAYS FOR NONDESTRUCTIVE EVALUATION AND ROBOT CONTROL	
12. PERSONAL AUTHOR(S): B.A. Auld and M. Gimple	
13a. TYPE OF REPORT: Annual; 13b. TIME COVERED: FROM 9/1/85 TO 8/31/86	14. DATE OF REPORT (Yr., Mo., Day): October 1986; 15. PAGE COUNT: 16
16. SUPPLEMENTARY NOTATION: The views and conclusions contained in this document are those of the authors and should not be interpreted as necessarily representing the official policies or endorsements, either expressed or implied, of the AFOSR or the U.S. Government.	
17. COSATI CODES — FIELD / GROUP / SUB. GR.	18. SUBJECT TERMS (Continue on reverse if necessary and identify by block number): Sensors, Robotics, Capacitive, Arrays, Distance Ranging, Edge Detection, Response Optimization, Field Adaptation, Pattern Matching, Matched Filtering, Analytic Modeling.

19. ABSTRACT (Continue on reverse if necessary and identify by block number)

Capacitive sensor arrays have been developed for multifunction sensing in robotic applications. The arrays consist of one-dimensional arrays of strip electrodes. They can be addressed to provide the different functions enumerated in 18. Distance ranging, edge detection, response optimization, and matched filtering have all been demonstrated experimentally with metal samples. Edge detection has been observed with dielectric samples, which cannot be sensed with inductive probes.

20. DISTRIBUTION/AVAILABILITY OF ABSTRACT: UNCLASSIFIED/UNLIMITED ☒ SAME AS RPT. ☐ DTIC USERS ☐	21. ABSTRACT SECURITY CLASSIFICATION: Unclassified
22a. NAME OF RESPONSIBLE INDIVIDUAL: B. A. Auld	22b. TELEPHONE NUMBER (Include Area Code): 767-4933, (415)723-0264; 22c. OFFICE SYMBOL: NE

DTIC ELECTE NOV 26 1986 D

DD FORM 1473, 83 APR — EDITION OF 1 JAN 73 IS OBSOLETE.

Unclassified
SECURITY CLASSIFICATION OF THIS PAGE

DTIC FILE COPY

AFOSR-TR- 86-1073

ELECTROMAGNETIC SENSOR ARRAYS FOR NONDESTRUCTIVE EVALUATION AND ROBOT CONTROL

by

B. A. Auld and M. Gimple

Annual Report
on research performed under
Contract : F49620-84-C-0095
Principal Investigator
B. A. Auld

Edward L. Ginzton Laboratory
W.W. Hansen Laboratories of Physics
Stanford University
Stanford, California 94305

October 1986

I. Objectives of the Research

Over the three-year period of the proposed research, modeling, analysis, design, and concept-testing experiments will be carried out at Stanford University to establish a scientific base and design philosophy for electromagnetic sensor arrays. Both inductive (eddy-current) and capacitive sensors will be studied. Applications goals are nondestructive evaluation and robot control. This research will be coordinated with a closely related effort proposed by SRI International. The specific schedule of tasks is summarized as follows:

First Year : Field-, interaction-, and system-models will be analyzed for rudimentary (2-element) sensors. Concepts will be tested experimentally.

Second Year : One-dimensional scanned and staring modeling will be developed and specific designs generated for scanned arrays.

Third Year : Specific designs will be generated for staring arrays, and modeling of two-dimensional arrays will be developed.

II. Status of Research Effort

(a) Introduction

Electromagnetic arrays have been used effectively for many years in optimizing the responses of antenna systems. The basic principles that make arrayed antennas work and make them easy to control can also be applied to near-field electromagnetic array sensors. The array factor allows for flexibility in sensor geometry. Firstly, by exciting only a portion of an array in a sequential fashion one can physically scan and interrogate a region of a sample without having to move the sample or the probe head itself. Secondly, the field configurations can be altered by selectively exciting electrodes of an array. Also, the information received can be selected by combining electrodes to form different effective receiver geometries. Thirdly, array configurations allow for real-time analog signal processing. For instance, one can perform pattern matching by choosing the spatial resolution of the probe to match the spatial resolution of the desired feature.

The electromagnetic basis of the sensor allows for multi-parameter sensing. First, one can measure distance of the probe from an object by measuring probe electromagnetic coupling with the sample object. Second, the existence and size of flaws can be determined

by measuring changes in voltage versus current characteristics at the probe terminals. Thirdly, simple surface features such as edges can be located by using differentially connected probe pairs. Finally, material properties such as dielectric constant and conductivity can be extracted by measuring changes in capacitances and resistances in known geometry samples.

Electromagnetic sensor arrays come in two versions: capacitive and inductive. Capacitive probes are the focus of this paper. Inductive probes are discussed in a companion paper [1] by researchers at SRI.

(b) Sample Materials

Capacitive probes can be used to investigate the properties and structure of both metals and dielectrics. For metals only surface features can be extracted. Charges which accumulate at the surface blind the capacitive probe to interior structures. Dielectrics fortunately do not have this problem. Both surface and interior features can be examined.

(c) Probe Capabilities

Reference [2] discusses different capacitor array configurations and the capabilities that one can get from such sensing systems. In this paper we demonstrate four such basic capabilities with slight modification:

Distance Ranging

Edge Detection

Response Optimization (Field Adaptation)

Pattern matching (Filtering)

(d) Basic Probe Element

The basic probe element is shown in Fig. 1(a). It is essentially a parallel plate capacitor that has been opened up such that the two plates lie in the same plane against a common substrate. The electric field lines rather than being parallel (uniform) are now elliptical (non-uniform). The probe is operated by applying a voltage to one electrode and measuring the current to ground from the second electrode (receiver). Interrogated samples are placed in the lower half space. Changes in measured current reflect changes in the sample-probe system configuration. A metal sample, which is grounded, when placed close to the the

electrodes will shunt current around the receiver electrode to ground and thus lower the output signal. Dielectrics on the other hand will enhance the output for they increase the capacitive coupling between the sensing electrodes, without shunting any significant current to ground.

For a single port eddy current device we know [3] that the change in impedance is given by

$$\Delta Z = \frac{j\omega\mu_o}{I^2}\int\left(\left\{\frac{\partial}{\partial z}\phi\right\}\phi' - \phi\left\{\frac{\partial}{\partial z}\phi'\right\}\right)dxdy \tag{1}$$

where ϕ is the magnetostatic potential ($H = \nabla\phi$) and the integration is performed over the surface of the mouth of the flaw. The primed notation refers to those quantities that exist in the presence of the flaw. The unprimed quantities refer to flaw absence. For the capacitive device described above we have a dual relationship. That is,

$$\Delta Y = \frac{j\omega\epsilon_o}{V^2}\int\left(\psi\frac{\partial\psi'}{\partial z} - \psi'\frac{\partial\psi}{\partial z}\right)dxdy \tag{2}$$

ψ is the electrostatic potential ($E = -\nabla\psi$) and the integration is performed over the surface of the test piece. Solutions for simple geometries can be extracted directly. For more complex geometries approximations and numerical techniques must be employed.

Figure 1(b) shows a similar configuration to that in Fig. 1(a) except that the source now consists of two contiguous, elementary electrode fingers excited simultaneously and the receiver consists of two contiguous, elementary electrode fingers whose currents' outputs are added together. As shown in the figure this allows for deeper field penetration and higher sensitivity at a given distance away.

Experiments demonstrating this effect were conducted using these probes with metallic samples. The electrodes that were used are 40 mils wide and 475 mils long. They are separated by 50 mils. A full array of electrodes were employed (8 to 9 fingers) even though only a subset was actively involved in the measurements. The remaining electrodes were explicitly grounded. Experimental results are shown in Fig. 2. In order that the two geometries could be compared on a similar basis both outputs were nomalized to a 0 dB level at the zero vertical distance position. Note that the the curve for the two-finger scaled probe dominates over that for the 1-finger scaling case. This is an indication that the fields do penetrate further into the interrogation region when the effective electrode

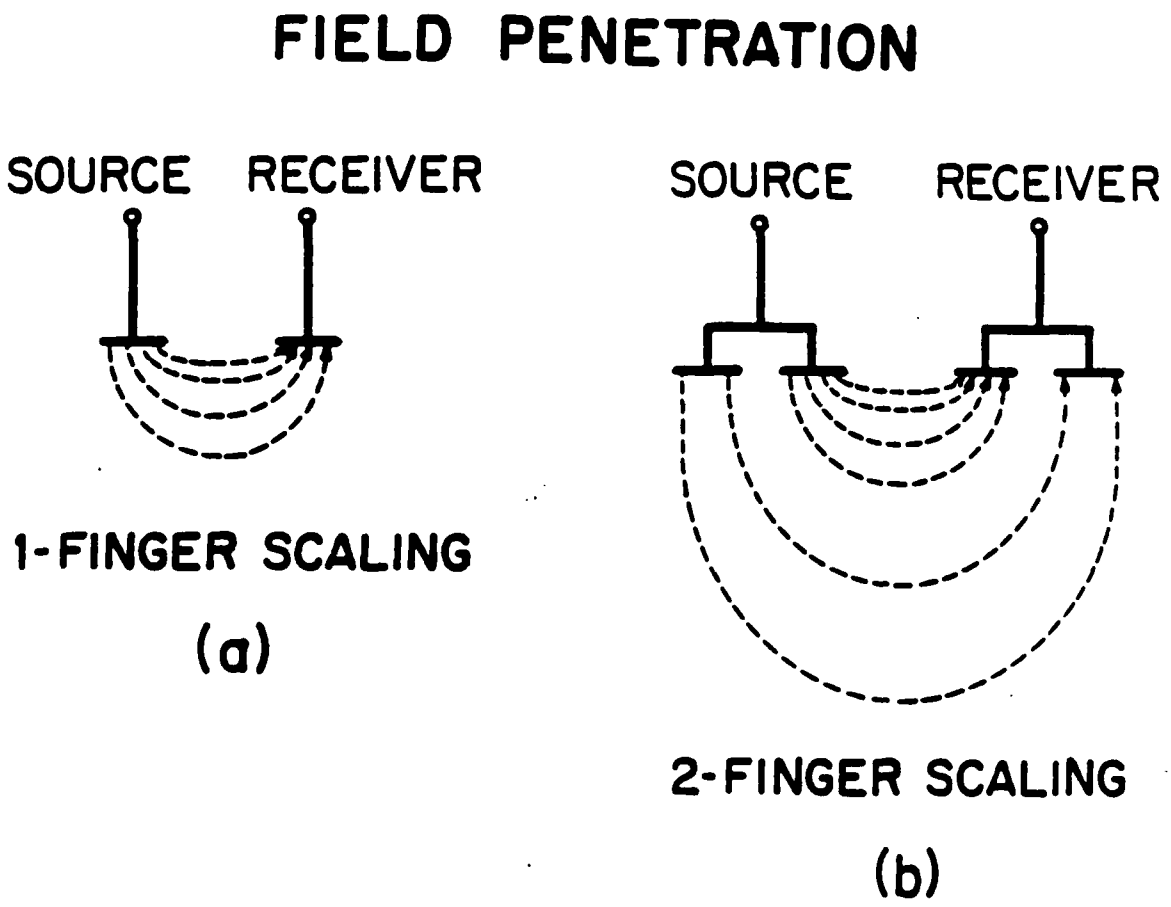

Figure 1

Elementary capacitive probes. They are used for distance ranging.

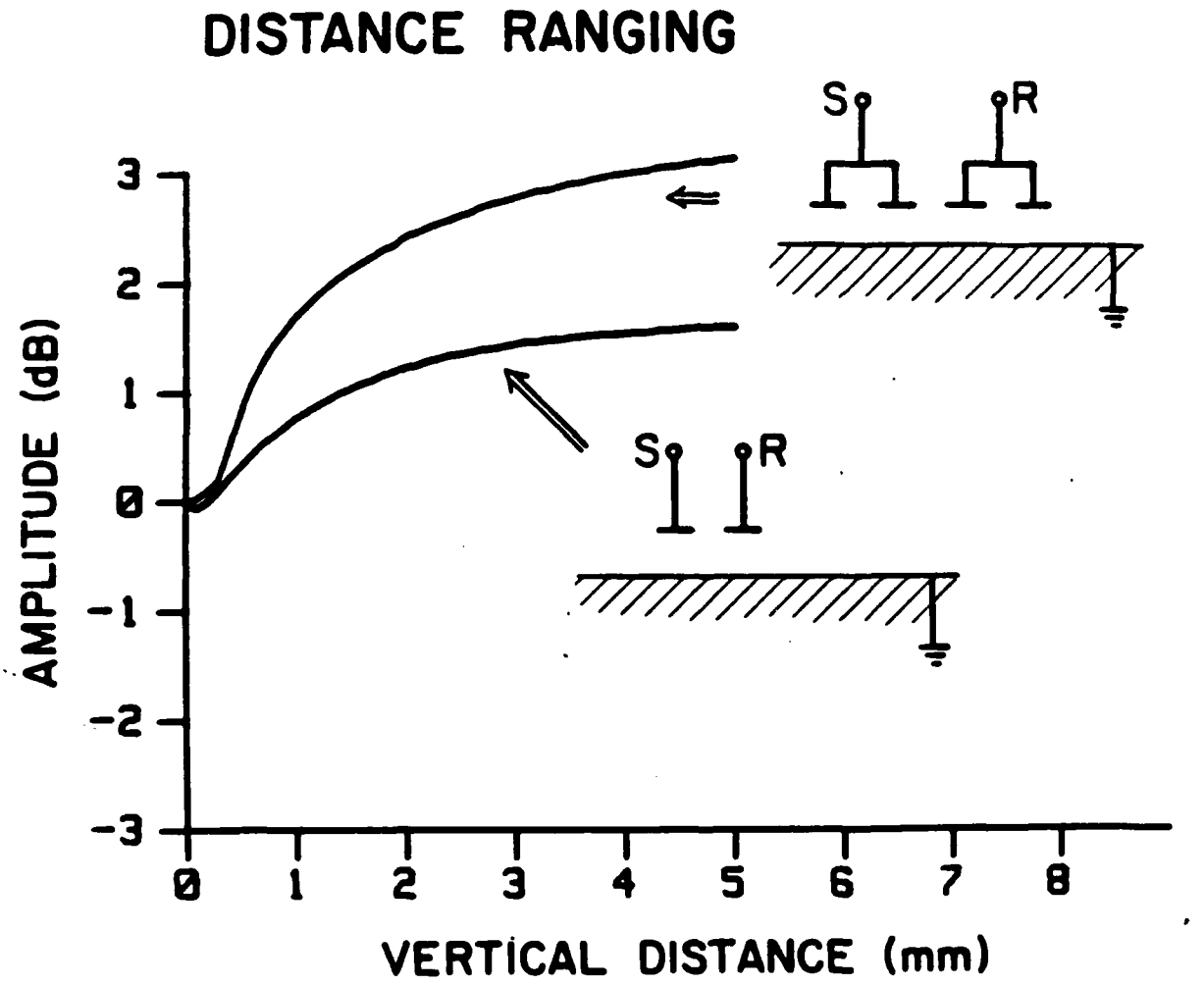

Figure 2

Normalized distance ranging output for the two elementary capacitive probes.

widths are increased. Also note that for extremely small vertical distances the sensitivity of the probes to distance (slope) is small. This is due to the fact that at small distances the metal sample is so close to the source electrodes that it completely shields the receiving electrode from any interaction.

(e) Complex Electrode Configurations

The configurations of Fig. 1 are sensitive to both vertical distances and horizontal displacements. Separating the two effects from each other is not readily done with a two-electrode probe. Thus, there is a need to adopt a probe geometry having a greater number of source/receiver electrodes. Figure 3 displays electrode configurations that make use of multiple source/receiver electrodes, with differential electronics to eliminate signals from common mode effects. Changes that affect both sides of the differential pair similarly (such as changes in vertical distances) are nulled. Only changes that disturb parts of the probe fields will result in non-zero outputs. Figure 3(a) is the simplest differential configuration. It is essentially two elementary probes connected in tandem with opposite polarity.

Experimental results for a grounded metal, slotted sample are shown in Fig. 4. The slots are 0.75 inches wide and 10 mils and 5 mils deep, respectively. The sample is scanned in a direction perpendicular to the sample slots. The probe is oriented such that the scan direction is perpendicular to electrode fingers. The peaks and valleys in the signal correspond to the edge components of the slots. A point to note is that the response to the deeper slot is larger than the response to the shallower slot. Thus, the probe is sensitive to slot depths. Also note that the response for a given depth slot is not symmetric for each edge (i.e. the size of the peak does not equal the size of the valley). This is due to the fact that the differential electronics is not balanced to zero. This purposeful asymmetry in gain paths allows us to measure output signal polarity from the signal amplitude alone.

Figure 5 displays results for a dielectric sample. The sample used is Delrin (ϵ_r=3.7). The three slots are 0.625 inches wide and 20 mils, 10 mils, and 5 mils deep, respectively. Note, that in the dielectric case a peak (valley) in the output signal occurs where a valley (peak) would occur with a metal sample. Also, one should note that the probe's sensitivity to each of the dielectric slots is the same (each peak and valley is of approximately the same size). We infer from this that the probe's sensitivity reaches saturation at a point

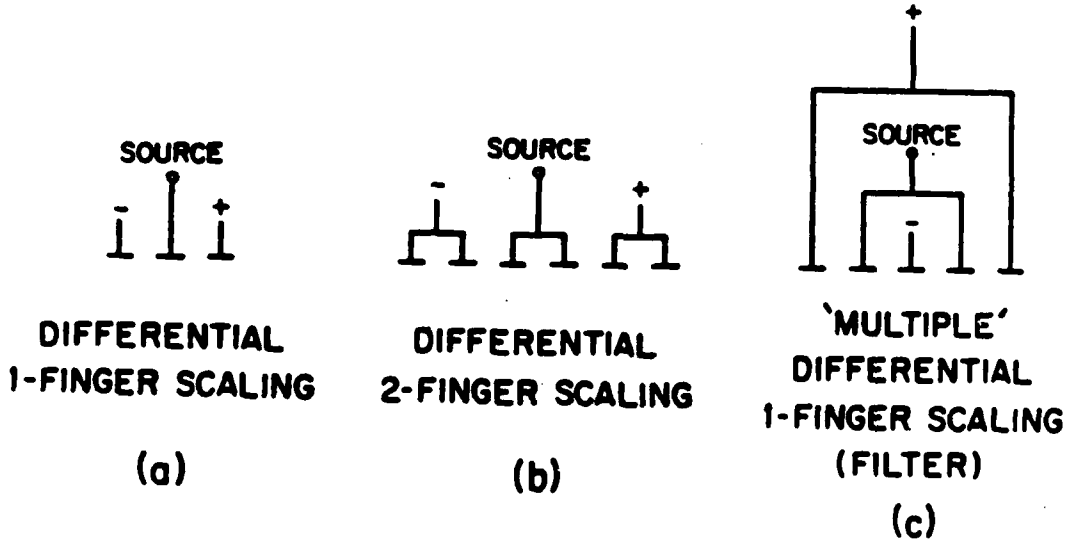

Figure 3

Three complex electrode probe configurations. They are used to extract lateral surface features.

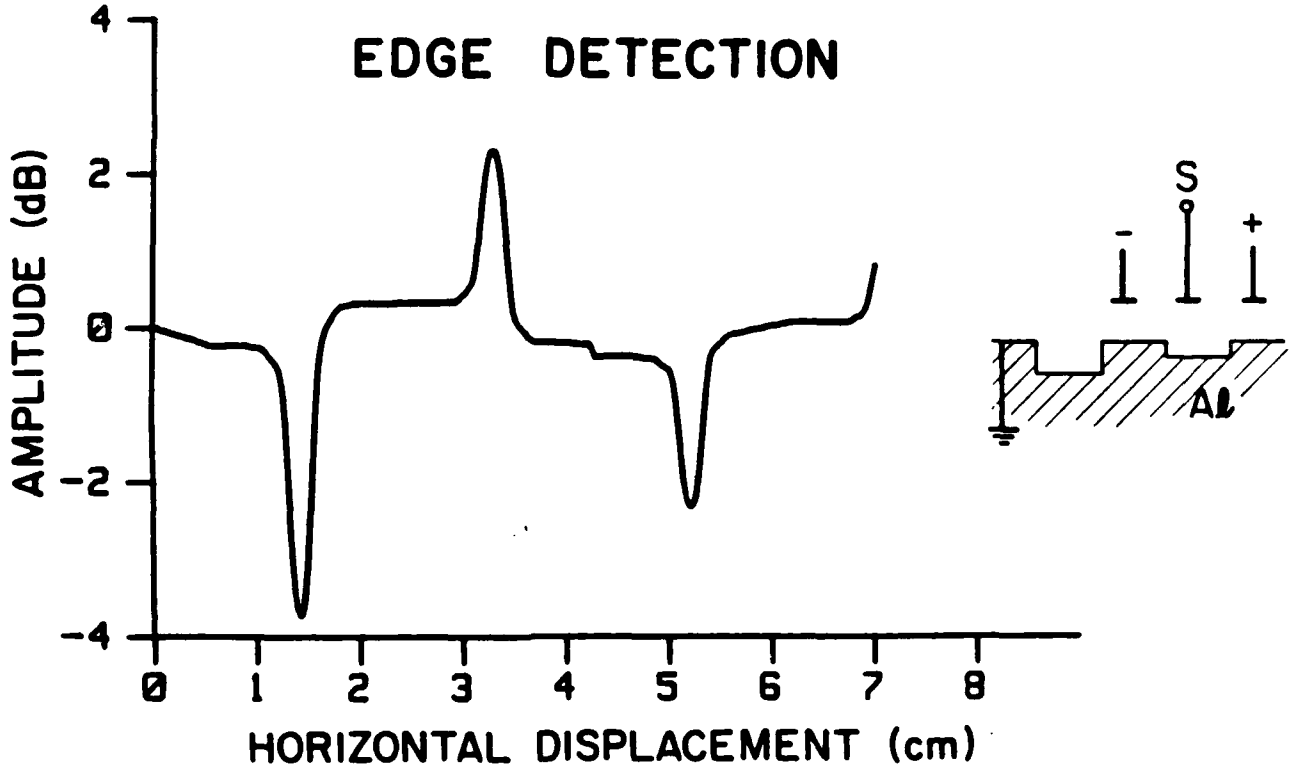

Figure 4

Horizontal scan of a slotted A1 sample with a 1-finger scaled differential probe. The slot depths are 10 mils and 5 miles, respectively. The sample is explicitly grounded.

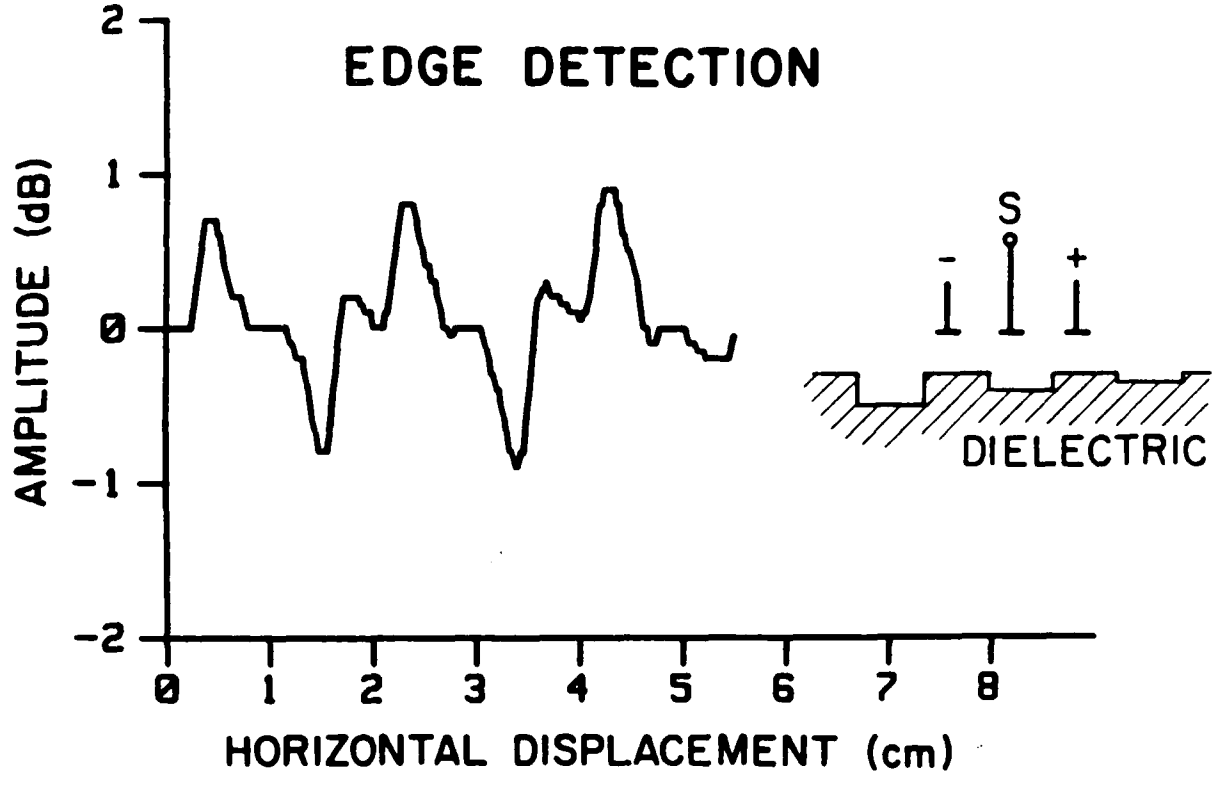

Figure 5

Horizontal scan of a slotted Delrin sample with a 1-finger scaled differential probe. The slot depths are 20 mils, 10 mils, and 5 mils, respectively.

under 5 mils deep. Further investigation is needed here.

Figure 3(b) displays a configuration similar to Fig. 3(a) save for the fact that 2-finger scaling is employed. One should expect better sensitivity but lower horizontal resolution than in the 1-finger scaling case. The lower horizontal resolution is due to the fact that an edge disturbance starts to cause a mismatch as it starts passing over the receiver electrodes, and reaches maximum mismatch when the edge is centered on the source electrode. Since 2-finger scaling probes are physically larger, then the peaks and valleys in the signals will be wider. Experimental results are displayed in Fig. 6.

The third differential probe consists of two single differential probes connected in tandem with the opposite polarity (see Fig. 3(c)). The purpose of this probe configuration is to look at two features (edges) simultaneously that are separated in space (filtering). When the spatial separation of the sample edges matches the spatial separation of the source electrodes then the output signal will be the sum of two edge signals overlapping giving a large peak or valley. At any other slot width the output signal tends to separate into two smaller individual signals. The degree of separation is dependent not only on the slot width itself but also on the width of the impulse response of the probe. Figure 7 displays experimental results for this probe scanned over three slots of widths of 0.180 inches (matched) 0.125 inches, and 0.500 inches, respectively in explicitly grounded metal sample.

To apply capacitive probes to quantitative nondestructive evaluation and intelligent robot sensing, it is necessary to quantitatively interpret the probe signals. This requires the development of probe interaction modeling based on Eq. (2). In investigating the behavior of long arrays, one can first approximate the probe as though it is of infinite extent. For an infinite array the analytical solution for the electric fields in the interrogating half-space without any samples present is given by [4]. The solutions are in the form of summations of Legendre polynomials. We are investigating the area of using perturbation methodologies to extract the field expressions that occur when sample objects are present with and without surface features such as edges and slots. This is an area of future work, and will be extended using finite difference calculations for the various probe geometries discussed above.

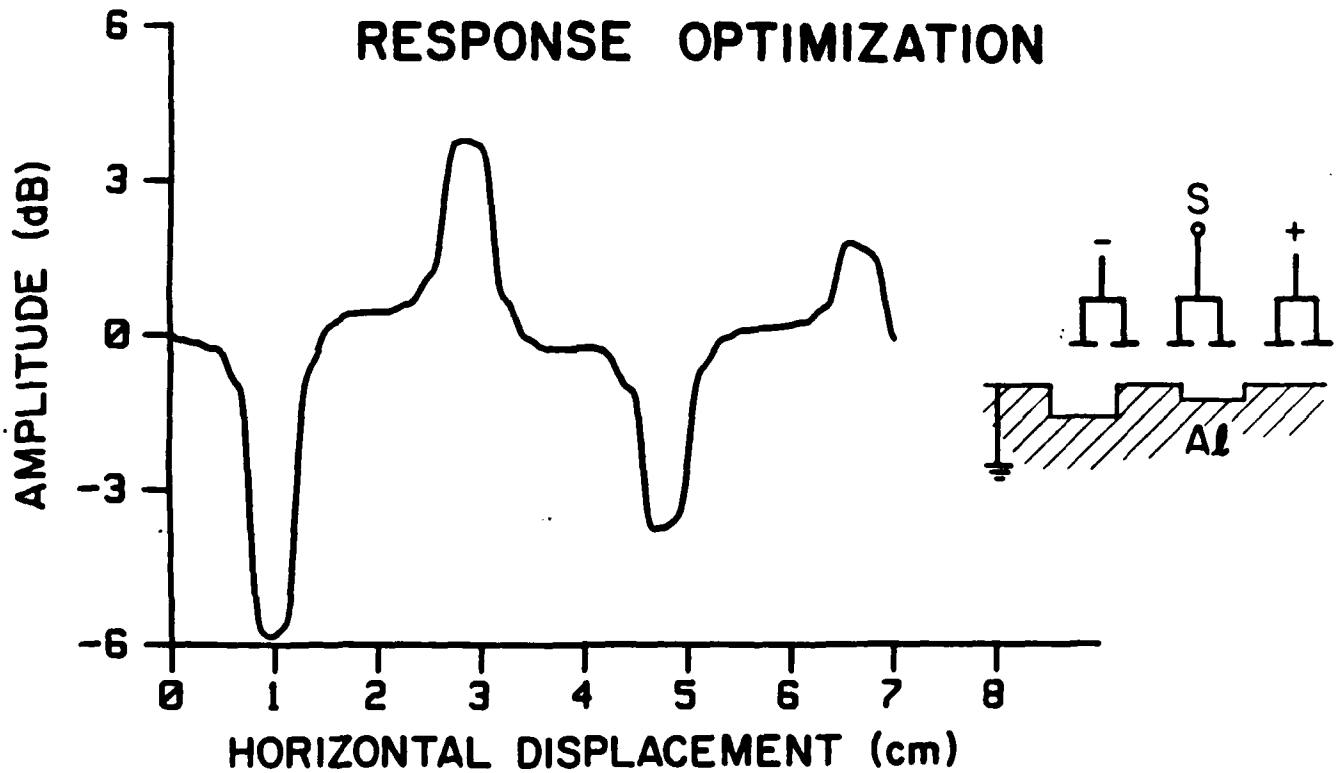

Figure 6

Horizontal scan of a slotted A1 sample with a 2-finger scaled differential probe. The slot depths are 10 mils and 5 mils, respectively. The sample is explicitly grounded.

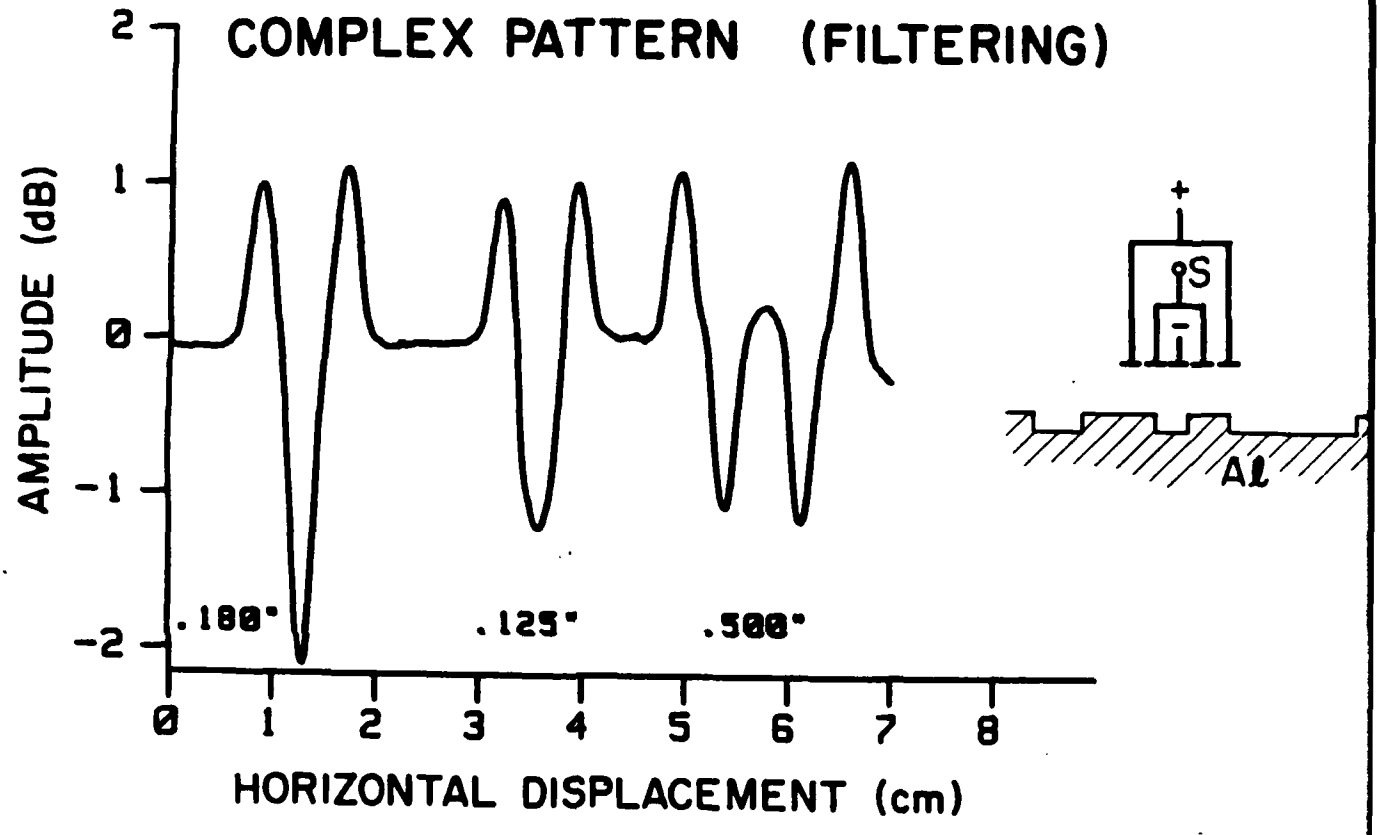

Figure 7

Horizontal scan of a slotted A1 sample with a spatial filter probe. The slots are 20 mils deep and are 0.180 inch (matched), 0.125 inch, and 0.500 inch wide, respectively. The sample is explicitly grounded.

(f) Conclusion

Four basic capabilities of capacitive arrays have been demonstrated. Also it has been demonstrated that capacitive arrays can be effective for both metals and dilectrics.

Future plans involve developing more analytical modeling capacity in order to produce better probes and to eliminate the need for recalibration for new sample geometries. Considerations for future probes include extending array geometries into 2-D and incorporating microelectronic preamplification in close proximity to the measuring electrodes.

(g) Acknowledgements

We would like to thank A. J. Bahr and A. Rosengreen at SRI International for their close collaboration.

References

1. A. J. Bahr and A. Rosengreen, "Inductive Sensor Arrays for NDE and Robotics," to appear in *Proceedings of Annual Review on Progress in Quantitative Nondestructive Evaluation*, La Jolla, California, August 4–8, 1986.
2. B. A. Auld, J. Kenney, and T. Lookabaugh, "Electromagnetic Sensor Arrays-Theoretical Studies," in *Review of Progress in Quantitative Nondestructive Evaluation 5A*, D. O. Thompson and D. E. Chimenti, eds., Plenum Press, New York (1985).
3. B. A. Auld and S. Jefferies; J. C. Moulder and J. C. Gerlitz, "Semi-Elliptical Surface Flaw EC Interaction And Inversion Theory," in *Review of Progress in Quantitative Nondestructive Evaluation 5A*, D. O. Thompson and D. E. Chimenti, eds., Plenum Press, New York (1985).
4. D. P. Morgan, *Surface-Wave Devices for Signal Processing*, Elsevier Science Publishers, Amsterdam (1985) pp. 335-361.

III. List of Publications

B. A. Auld, J. Kenney, and T. Lookabaugh, "Electromagnetic sensor arrays–Theoretical Studies," in *Review of Progress In Quantitative Nondestructive Evaluation 5A*, D. O. Thompson and D. E. Chimenti, eds., Plenum Press, New York (1985); pp. 681-690.

B. A. Auld and A. J. Bahr, "A Novel Multifunction Robot Sensor," in *IEEE Proceedings of the 1986 International Conference on Robotics and Automation*, San Francisco, IEEE Computer Society Press, Washington (1986); pp. 1791-1797.

M. Gimple and B. A. Auld, "Capacitive Arrays for Robotic Sensing," to appear in *Proceedings of the La Jolla Review of Progress in Quantitative Nondestructive Evaluation*, La Jolla, California, August 4–8,1986.

IV. Professional Personnel

B. A. Auld, Principal Investigator

M. Gimple, Graduate Student

V. Interactions

B. A. Auld and A. J. Bahr, "A Novel Multifunction Robot Sensor," presented at the 1986 International Conference on Robotics and Automation, San Francisco, April 14-17 1986.

M. Gimple and B. A. Auld, "Capacitive Arrays for Robotic Sensing," presented at the Review of Progress in Quantitative NDE, La Jolla, California, August 1986.

VI. New Discoveries

A novel capacitive array for robotic sensing has been designed, built and partially tested. We have demonstrated (1) distance ranging, (2) edge detection, (3) response optimization (field adaptation), and (4) pattern matching, with this probe.

A NOVEL MULTIFUNCTION ROBOT SENSOR

by

B.A. Auld
Stanford University

and

A.J. Bahr
SRI International

To be presented at
1986 IEEE International Conference on Robotics and Automation
San Francisco, California
April 7–10, 1986

Edward L. Ginzton Laboratory
W.W. Hansen Laboratories of Physics
Stanford University
Stanford, California 94305

January 1986

A NOVEL MULTIFUNCTION ROBOT SENSOR

B. A. Auld
Edward L. Ginzton Laboratory
Stanford University
Stanford, CA 94305

A. J. Bahr
SRI International
Menlo Park, CA 94025

ABSTRACT

This paper describes a novel five-coil eddy current probe with the capability of simultaneous multifunction sensing, suitable for automated manufacturing and sensing. The probe consists of a single drive coil with two pairs of smaller pickup coils. Multiple sensing functions are realized by reading the pickup coils in different combinations of operation, and experimental results are given for position and angle sensing of shallow steps on a metal surface.

INTRODUCTION

This paper describes the design and testing of a new type of electromagnetic sensor capable of providing the following robot sensing functions:

(1) proximity,

(2) edge position and orientation,

(3) tactile,

(4) material diagnosis,

(5) flaw location and sizing,

for automated manufacturing and inspection. Inductive probes have been used for some time in robotics for proximity sensing and for weld seam tracking. However, little use has been made of the sophisticated design concepts, developed for quantitive nondestructive evaluation (NDE) in recent years.[1-4] Application of this existing technology to robot sensing constitutes the goal of this work, which aims to develop a new generation of EM sensors. This technology has not yet been applied to robotics, even though electromagnetic sensors (both inductive and capacitive) are often preferred over full-scale vision because of their speed in providing specific information without elaborate signal processing. Inductive sensors also offer advantages over vision and photoelectric-fiber sensors in opaque environments (such as in machine tool sensing under a jet of cooling fluid) and over acoustic sensors in outer space applications.

Electromagnetic sensors are often criticized because it is felt that:

(1) They are incapacitated by ambient electrical noise,

(2) They are uncalibrated for proximity measurement, unless the material properties of the object are known, and

(3) They have inadequate spatial resolution.

However, by using and extending existing NDE technology these presumed difficulties can be overcome. The solutions are as follows:

(1) Problems of electrical interference can be handled by suitably choosing the excitation frequency of the probe and using electrical filtering. Since the probe structures are physically small they can be operated at very high frequencies, while still functioning in a nonradiating (or quasistatic) mode. Inductive sensors of special types have been successfully operated at frequencies above 1000 MHz,[5] where interference from factory machinery noise is completely negligible.

(2) It is true the proximity signal generated by an electromagnetic sensor does depend on the material properties of the object. However, the sensor signal contains both amplitude and phase information, and from this data it is possible to extract both the material properties and the proximity distance. This is a technique commonly used in NDE.

(3) The interrogating field of the sensor, because it is quasistatic, extends only to a distance comparable to its dimensions. The spatial resolution can be further enhanced by suitably configuring the sensor geometry. In this situation the sensor functions analogously to an optical spatial filter, although it is a nonradiating device operating at a much lower frequency. Application of signal processing techniques from radar and sonar technology can also be used to enhance sensor performance.

As robot sensors, inductive (or eddy current) sensors can be used individually or in one- and two-dimensional arrays. They offer fast electronic

scanning without mechanical motion, selective analog detection of desired object features, and even (when modified as described below) both tactile and proximity sensing in the same device.[5,7]

GENERAL THEORY OF INDUCTIVE SENSORS

Figure 1 illustrates symbolically two of the most frequently used types of eddy current probes for nondestructive evaluation. Part (a) shows an absolute sensor, consisting of a single coil scanned over a workpiece. The measured signal is the magnitude, and phase of the change in coil impedance ΔZ, produced when the probe passes over the flaw. Both the amplitude and phase parts of the signal contain significant information, used in characterizing and sizing the flaw. This process is now well-understood and an extensive literature is available.[1-4] In Fig. 1(a) the flaw detection process can be pictured by imagining a flawed workpiece placed in the fringing magnetic field around the coil. If the workpiece is scanned under the coil, while keeping its proximity distance constant, the resistance and reactance of the coil changes as the flawed part of the workpiece passes under it. It is this change in impedance signal (ΔZ) that is used in locating and sizing the flaw. Changes in the proximity distance between the workpiece and the coil also have the effect of changing the coil impedance. Since the workpiece has a much larger volume than the flaw, changes in the proximity distance produce a much larger ΔZ than does the flaw itself. This is a serious inconvenience in NDE, but it is what makes an inductive probe such a sensitive proximity sensor for robotics.

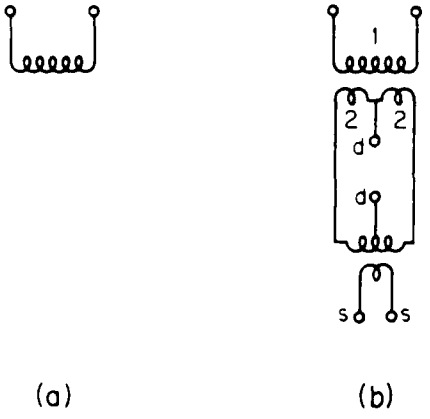

Fig. 1. Two common types of inductive sensors. (a) Absolute, (b) Reflection.

In NDE a number of methods have been developed for suppressing the unwanted proximity signal. Figure 1(b) shows a special sensor geometry developed for this purpose. This sensor, called a reflection probe, consists of a single drive coil 1 and two pickup coils 2,2, which are read differentially. It is illustrated in the figure by picturing the pickup coils as the two halves of a center-tapped transformer secondary. The difference signal from the two pickup coils is read at the terminals dd in the figure. If the workpiece is again imagined to be placed near the transformer coils the magnetic coupling between the primary and secondary windings is changed. When the workpiece is unflawed, changes in the proximity distance between the probe and the workpiece produce equal changes in coupling between the primary coil and each part of the secondary. At the difference terminals dd in the figure these changes cancel out. The probe is therefore insensitive to changes in proximity distance. However, changes in transformer coupling due to the presence of a flaw, which is localized in space, produce different changes in coupling to the two halves of the secondary, depending on the position of the flaw relative to the pickup coils. As the flaw passes first under one pickup coil and then under the other, a flaw signal with high spatial resolution and sensitivity is generated. It will be seen below that this type of sensor can also be used to detect the proximity signal, by reading the output at the sum terminals shown in the figure. In the reflection-type probe, the measured signals depend on changes in the transfer impedances (ΔZ_{21d} and ΔZ_{21s}) of the circuit in Fig. 1(b).

A general formulation of ΔZ theory has been developed for the two types of probes illustrated in Fig. 1. In the absolute probe

$$\Delta Z = \frac{1}{I^2} \int (E_1' \times H - E \times H') \cdot \hat{n} \, dXdY \qquad (1)$$

where, as shown in references 1 and 3, the integral is over the surface of the workpiece when the flaw is a surface-breaking crack. The unprimed fields under the integral are those produced by the probe at the workpiece surface in the absence of the flaw and the primed fields are those in the presence of the flaw. They are defined as the fields generated by applying a current I at the input terminals of the probe, and $\hat{n}$ is the exterior unit normal to the workpiece surface. For the reflection-type probe of Fig. 1(b), the corresponding ΔZ formula is[5]

$$\Delta Z_{12} = \frac{1}{I^2} \int (E_1' \cdot H_2 - E_2 \cdot H_1') \cdot \hat{n} \, dXdY \qquad (2)$$

where, again, the unprimed fields are for the unflawed workpiece and the primed fields are for the flawed workpiece. The subscripts on the fields indicate that they are excited by current I at terminals 1 and 2 in Fig. 1(b). Terminals 1 and 2 in the figure are defined as those exciting coils 1 and 2, respectively. For calculating ΔZ_{21d}, current I is applied at the difference output terminal, while ΔZ_{21s} is obtained by applying I to the sum terminals. Calculations using Eqs. 1 and 2 can be repeated for various positions of the probe relative to the flaw, giving a profile of the flaw signal obtained by scanning the probe past

the flaw.

THEORETICAL BASIS FOR PROXIMITY SENSING

The ΔZ formulas given above can also be used to calculate the proximity signal of an eddy current probe. In this case the unprimed fields in Eqs. 1 and 2 are defined as the fields produced at the workpiece surface when the probe is at a particular distance from the surface. The primed fields are those produced at the surface when the probe is at a greater distance. In this calculation the integral is performed over a surface corresponding to the top of the workpiece in its unprimed position, and the probe is always maintained in a fixed position relative to this surface. When the workpiece is moved to its primed position, further away from the probe, its surface lies below the original unprimed surface. This relationship is illustrated at the left side of Fig. 2, where the dashed line represents the unprimed position of the surface. The probe is maintained at a fixed position above this surface in evaluating both the unprimed fields at the original unprimed position of the workpiece surface, and the primed fields at the primed position of the workpiece surface (shown below the dashed line in the figure).

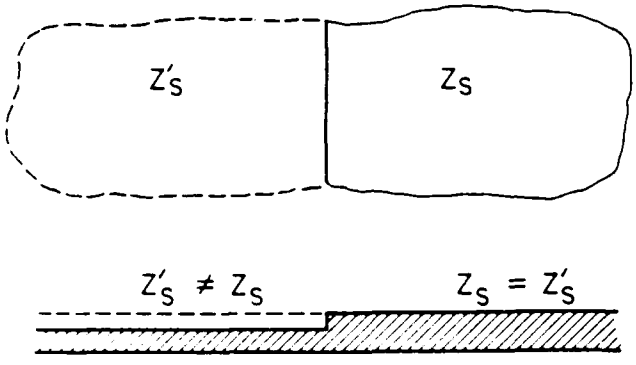

Fig. 2. Test sample for edge sensing experiments.

A detailed analysis of the eddy current proximity effect, called the lift-off effect in nondestructive testing, is given in references 8, 9 and 10. In the general treatment, spatial Fourier transforms are taken of the probe fields and the ΔZ integrals are rewritten in Fourier transform space, using the electromagnetic surface impedance Z_s at the workpiece surface for each Fourier component. It is found that for probe dimensions much larger than the electromagnetic skindepth in the workpiece material, a typical situation with highly conducting workpieces at frequencies above a few hundred kHz, Z_s is essentially constant over most of the spatial Fourier spectrum. In this case a constant surface impedance approximation can be introduced into the spatial domain integrals for the proximity ΔZ, and Eqs. 1 and 2 for proximity sensing become

$$\Delta Z = \frac{1}{I^2} \int \Delta Z_s H \cdot H' \, dXdY \qquad (3)$$

and

$$\Delta Z_{21} = \frac{1}{I^2} \int \Delta Z_s H_1 \cdot H'_2 \, dXdY \qquad (4)$$

where ΔZ_s is the change in surface impedance between the initial and final positions of the workpiece surface.

PROTOTYPE MULTIFUNCTION SENSOR

At the left of Fig. 3 is shown a more realistic schematic of the reflection type sensor introduced in Fig. 1(b). This geometry gives high sensitivity for flaw detection. At the same time it cancels out changes in transmission from terminal 1 to terminal 2 due to changes in the proximity spacing between the probe and the workpiece. If, on the other hand, the pickup coils are connected to give a sum output, the output is very sensitive to the proximity spacing. Both difference and sum signals can be read at the same time using the output connections of Fig. 1(b). The difference output can then be used to identify and locate workpiece features such as edges, while the sum signal gives a measure of proximity. If a compliant dielectric layer is placed between the coils and the object, as shown in the figure, the sum signal will also give a measure of tactile pressure after contact is made with the object. Such tactile effects are actually observed in nondestructive evaluation probes, despite efforts to avoid them by rigid probe construction.

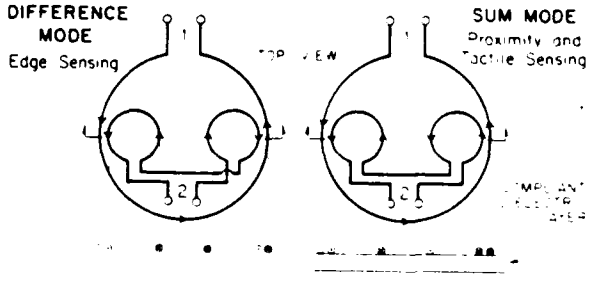

Fig. 3. Difference and sum mode readouts from a reflection sensor.

Figure 2 shows an aluminum workpiece with a shallow step, having a depth of a few thousandths of an inch milled into the upper surface. This was used to experimentally test the ability of the reflection type sensor at the left of Fig. 3 to detect the position and orientation of edges, and to compare measured sensor signals with theoretical predictions. When the stepped plate is placed under the reflection sensor the coupling between the drive coil and the pickup coils is determined by the position and the angular orientation of the edge of the step relative to the sensor. This effect can be analyzed by using Eq. (4) and integrating over the lefthand side of Fig. 2, where

$$\Delta Z_s = Z_s' - Z_s$$

is different from zero. The sensor signal due to the step is calculated as if it were simply a lift-off effect over part of the workpiece surface. This clearly neglects the effect of eddy current perturbation near the edge of the step, but comparison with experiment shows that the perturbation is not important in this case. When the edge is oriented parallel to the horizontal axis in Fig. 2, the changes in coupling for the two pickup coils are the same, and the signal cancels at the difference port. Orientation of the edge parallel to the vertical axis, however, gives different couplings into the pickup coils, and a net edge signal appears at the output port. This signal is maximum when the edge is midway between the two pickup coils. The probe is therefore sensitive to both position and orientation of the edge.

For a vertical edge, the sensor has maximum sensitivity to edge position and minumum sensitivity to edge orientation, and conversely for a horizontal edge. From these observations it follows that an ideal sensor for simultaneously detecting both the position and the orientation of an edge has the form shown on the left of Fig. 3, but with an extra set of pickup coils aligned vertically. For a horizontal edge the horizontal pair of pickup coils detects angle variations and the vertical pair of pickup coils detects position variations. Such a sensor is illustrated in Fig. 4, where coils 2 are for angle sensing and coils 2′ are for position sensing. With this type of sensor, search for an edge is performed by scanning over the plate until a signal appearing at output 2 or 2′ indicates the presence of an edge. The robot hand then rotates the sensor to null the signal at output 2 and moves along the axis of coils 2′ to maximize the signal at output 2′. At this point the hand and sensor is centered above the edge, with the axis of coils 2 aligned along the edge. Tracking the edge then proceeds by moving stepwise along the coil 2 axis, recorrecting the angular orientation of the hand after each advance when the edge being tracked is curved.

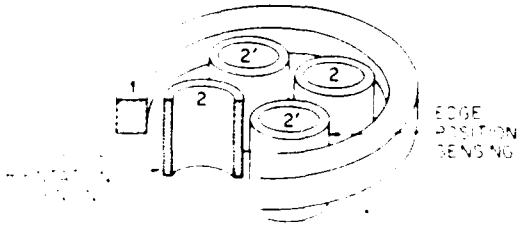

Fig. 4. Five-coil sensor for position and angle sensing of an edge. Coils 2′ are for position sensing; coils 2 for angle sensing.

For the very shallow edge used in our experiments (Fig. 2), ΔZ_2 in Eq. (4) is small and Z_s' and Z_s may be replaced by Z_1. This latter quantity is the field produced at the unstepped surface by current excitation at terminals 2. This reduces Eq. (4) to

$$\Delta Z_{12}(X_0,Y_0) = \frac{1}{I^2}\int \Delta Z_s(X,Y) \left\{H_1 \cdot H_2(X,Y,X_0,Y_0)\right\} dXdY \qquad (5)$$

where ΔZ_s, the difference between the primed and unprimed surface impedances, is zero on the right-hand side of Fig. 2. (It should be noted that the magnetic fields in Eq. (5) contain only components parallel to the surface of the test object.) The variables X_0 and Y_0 define the position of the center of the probe in a coordinate system in the plane of the surface. A final comment should be made about the form of Eq. (5). It is seen to have the form of a convolution integral, in which the scalar product of the coil fields H_1 and H_2 is the kernel. Figure 5 shows the form of this kernel, with $X_0, Y_0 = 0$, for the actual sensor used in the experiments (Fig. 6).

Fig. 5. Convolution kernel for edge sensing with a reflection type inductive sensor. A line through the positive and negative peaks corresponds to a horizontal line through the pickup coils in Fig. 3.

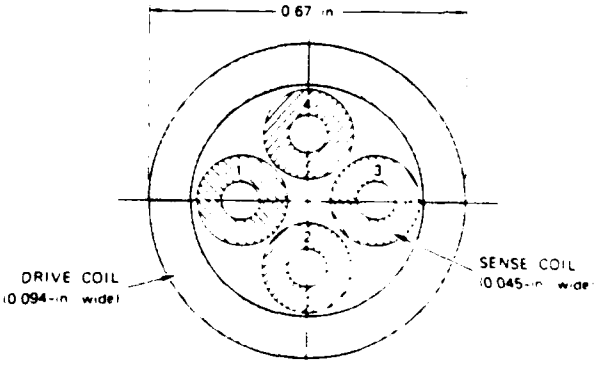

Fig. 6. Cross section of a five-coil reflection sensor.

MEASUREMENT SYSTEM

We have built an automated system for acquiring the amplitude and phase of a sensor's output voltage as the sensor is scanned in a plane (X and Y) under computer control (Fig. 7). The sensor array (or workpiece) can be stepped along in raster fashion in minimum increments of 0.002" (or multiples thereof). A Nortech NDT-18 eddyscope is used as source and receiver, and the digitized data are stored on magnetic tape for off-line processing. The NDT-18 eddyscope is an analog instrument containing a synthesized source that can be tuned from 50 Hz to 5 MHz and can be used with both absolute and reflection sensors. Software has been developed for displaying the data in several ways, including perspective plots and contour plots.

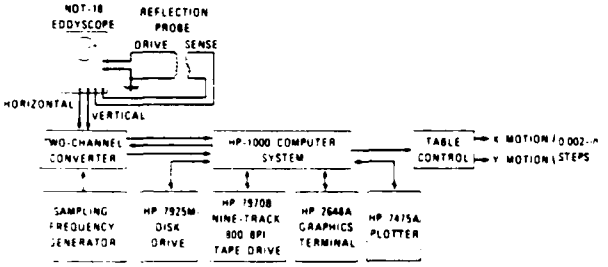

Fig. 7. Data acquisition system.

EXPERIMENTAL RESULTS

The five-coil air-core sensor described above, was designed at Stanford[5] and fabricated at SRI International.[7] For this prototype test the coils were made in a scaled-up form to minimize construction difficulties. The layout is shown in Fig. 6. The outer diameter of the drive coil is 0.67", and the outer diameter of each sense coil is 0.19". The centers of the diametrically opposed sense coils are separated by 0.28". Each sense coil contains 54 turns of #34 copper wire, while the drive coil contains 24 turns. This makes the height of each pickup coil 0.10", and the height of the drive coil 0.05". At 500 KHz the measured input impedance of the drive coil resting on an aluminum plate is 9.3 + j 17.4Ω, and the impedance of the differentially connected pickup coils is 5.6 + j 39.6, values compatible with the source and detector impedances of the NDT-18. Although the sensor contains two pairs of pickup coils, permitting the multifunction sensing operations described above, only one pair of pickup coils was used at a time in the experiments reported here. The aim has been to verify the edge angle and position sensing properties of this new type of sensor.

In one experiment, performed with the sensor centered over the edge in Fig. 2, the output of one pickup coil pair was measured as a function of the angular orientation of the pair axis with respect to the edge (Fig. 8). In the figure the small circles represent the sensor and the lines along the diameter denote the pair axis. A comparison is shown with the theory (black dots) of Eq. (5).

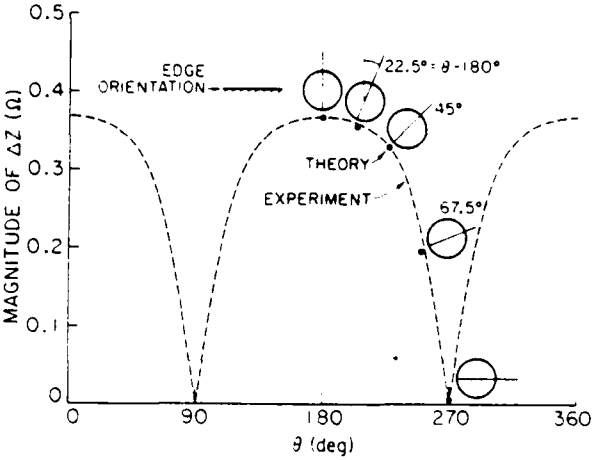

Fig. 8. Comparison of theory and experiment for edge angle sensing with the sensor of Fig. 6.

Although the experimental measurements were taken only at discrete angle values (as were the calculations), the results are shown, to avoid clutter in the figure, as a smooth curve fitting the data points. Theory and experiment were matched at one point because the measurement instrument was not calibrated for direct impedance measurement. A second experiment was made of the sensor output as a function of sensor position relative to the edge, for various angle orientations of the coil pair axis relative to the edge. In this experiment the five-coil sensor was used to make a series of five perpendicular scans across a 0.004" step in an aluminum plate. The orientation of the sensor differed in

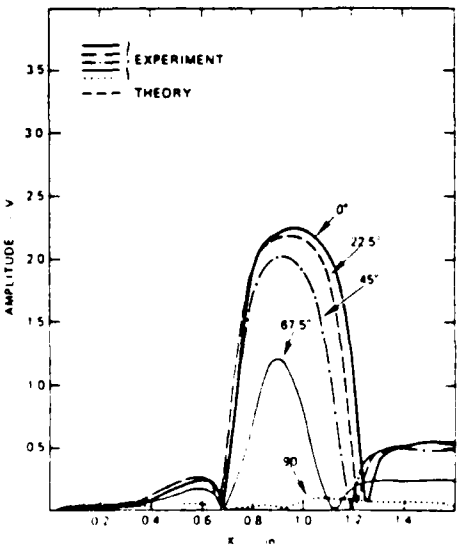

Fig. 9. Step response as a function of sensor orientation relative to the edge, at 500 kHZ.

each scan. Starting from the point at which the line through the centers of the differential pair of pickup coils was aligned with the scan direction (designated 0°), the sensor was rotated in steps of 22.5° through 90° (designated 90°). Experimental results are shown in Fig. 9. As expected, the maximum step response is obtained at 0°, and the response decreases as the sensor is rotated toward 90°. Comparisons with theory are shown for various rotation angles. Since the NDT-18 is an uncalibrated instrument, the theoretical and experimental data were matched at the maximum of the 0° scan. With this single point calibration, the shapes of the theoretical and experimental step responses are seen to agree well, and the peak amplitudes at other angles are in excellent agreement. The minor differences between theory and experiment outside the main step response are thought to be due to the perturbation of the eddy current pattern near the step edge, which is not included in the theory.

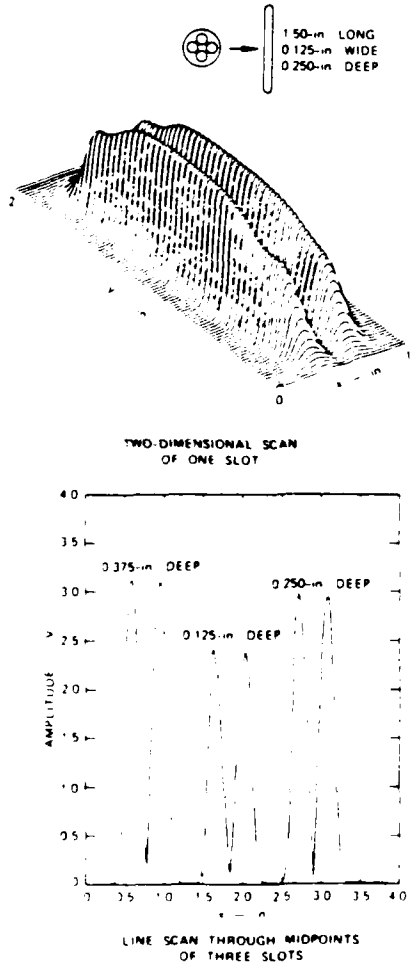

Fig. 10. Response of an NDE three-coil ferrite-core reflection probe to a shallow curved edge. Parallel orientation has the coil pair axis parallel to the scan direction and perpendicular orientation has it perpendicular to the scan direction.

For another experiment, three slots of different depths were milled into an aluminum plate. These slots were placed side by side, 1" apart and were all 0.125" wide and 1.5" long. Figure 10 shows the results of scanning across these slots with the five-coil sensor (only one pickup coil pair active). The perspective plot of the results obtained by scanning across the 0.250"-deep slot shows a typical differential response in the X-direction and a typical absolute response in the Y-direction. This is because the X-response is determined by the geometry of the pickup coil pair, while the Y-response is determined by the geometry of the drive coil. The line scan through the midpoints of these slots illustrates both the transverse resolution and the depth resolution of this sensor. The transverse resolution appears to be about ±0.125", and the depth resolution deteriorates rapidly for depths greater than 0.125". These numbers are consistent with the dimensions of the sensor and can be improved by reducing its size.

Figure 11 shows data taken by raster scanning a Nortech SPO-2065 ferrite nondestructive evaluation probe of reflection type over a curved step. The drive coil in this probe has an outer diameter of about 0.1". The pickup coil pair consists of two small D-shaped coils located side by side within the

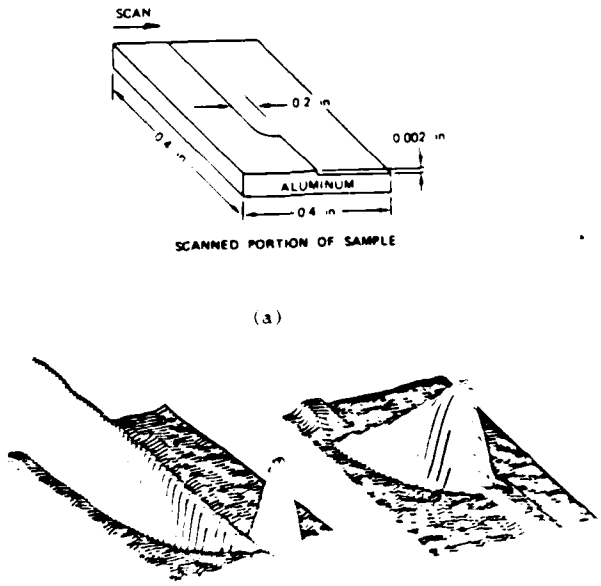

Fig. 11. Slot response of the five-coil reflection sensor at 500 kHz.
(a) Scanned Portion of Sample
(b) Parallel Polarization
(c) Perpendicular Polarization

inner diameter of the drive coil. Based on the dimensions of these pickup coils, a spatial resolution of about 0.040" is expected. A reflection sensor (or probe) in which the drive and pickup coils are essentially coplanar is linearly polarized; that is, the step response is maximum when the scan direction is perpendicular to the edge of the step and aligned with a line that passes through the centers of the pickup coils (parallel polarization), and it will be minimum when the sensor is rotated by 90° (perpendicular polarization). The response of the Nortech reflection probe to the curved edge illustrates this polarization-dependent behavior. The important implication of this characteristic is that, by combining data sets from both polarizations, the direction of an edge with respect to the scan direction can be determined. Thus, for example, by feeding this information back to a scan controller, the robot hand to which the sensor is affixed can be directed to follow an edge.

CONCLUSION

This paper has presented a comparison of experimental performance with theory for a novel five-coil inductive robot sensor. Although only the edge recognition and flaw detection functions have been tested experimentally, this device is also capable of simultaneous multifunction sensing (proximity, tactile, material properties diagnosis, flaw location, and flaw sizing). For the simple absolute type of inductive sensor (Fig. 1(a)) there exists a well-developed set of algorithms for flaw signal diagnosis, based on the concept of the flaw profile.[9,10] This concept is illustrated in Fig. 10 for the reflection type of sensor, where the flaw profile is measured along the crests of the signal printout. An analysis has been performed of reflection sensor-flaw interactions, and software is being prepared to implement a flaw sizing procedure for reflection sensors. Inductive sensors, in general, have a number of advantages over other categories of sensors (vision, photoelectric, acoustic, and capacitive). For example, unlike the other sensors mentioned, they are not disturbed by jets of cooling fluid in automated machining operations. This feature, coupled with an edge tracking capability, make the sensor described in this paper an attractive candidate for automated deburring operations. Other fabrication technologies are under active consideration for constructing inductive sensors and their capacitive duals, in both individual element and array configurations. The use of other technologies will be very important in realizing smaller-scale versions of the present sensor, in order to achieve a practically useful degree of spatial resolution.

ACKNOWLEDGEMENTS

This work was sponsored by the Air Force Office of Scientific Research under Contracts F49620-84-C-0095 and F49620-84-K-0011.

REFERENCES

[1] F. Muennemann, B.A. Auld, C.M. Fortunko, and S.A. Padget, "Inversion of eddy current signals in a nonuniform probe field," in Review of Progress in Quantitative Nondestructive Evaluation, 2, D.O. Thompson and D.E. Chimenti, eds., (Plenum, New York and London, 1983), pp. 1501-1528.

[2] J.R. Martinez and A.J. Bahr, "Statistical detection model for eddy current systems," in Review of Progress in Quantitative Nondestructive Evaluation, 3, D.O. Thompson and D.E. Chimenti, eds., (Plenum, New York and London, 1984), pp. 499-510.

[3] B.A. Auld, J. McFetridge, M. Riaziat, and S. Jefferies, "Improved probe-flaw interaction modeling, inversion processing, and surface roughness clutter, in Review of Progress in Quantitative Nondestructive Evaluation, 4, D.O. Thompson and D.E. Chimenti, eds., (Plenum, New York and London, 1985), pp. 623-634.

[4] B.A. Auld and S. Jefferies, "Semi-elliptical flaw EC interaction and inversion: Theory," presented at Review of Progress in Quantitative Nondestructive Evaluation, Williamsburg, Virginia, June 23-28, 1985.

[5] J.M. Prince and B.A. Auld, "Development of active ferromagnetic resonance signal probes and associated signal processing methods," in Review of Progress in Quantitative Nondestructive Evaluation, 3, D.O. Thompson and D.E. Chimenti, eds., (Plenum, New York and London, 1984), pp. 1369-1376.

[6] B.A. Auld, J. Kenney and T. Lookabaugh, "Electromagnetic sensor arrays--Theoretical studies," presented at Review of Progress in Quantitative Nondestructive Evaluation, Williamsburg, Virginia, June 23-28, 1985.

[7] A.J. Bahr, "Electromagnetic sensor arrays--Experimental studies," presented at Review of Progress in Quantitative Nondestructive Evaluation, Williamsburg, Virginia, June 23-28, 1985.

[8] M. Riaziat and B.A. Auld, "Eddy current probe design and matched filtering for optimum probe design," in Review of Progress in Quantitative Nondestructive Evaluation, 2, D.O. Thompson and D.E. Chimenti, eds., (Plenum, New York and London, 1983), pp. 189-204.

[9] B.A. Auld and M. Riaziat, J. Appl. Phys. vol. 54, p. 3509 (1983).

[10] M. Riaziat, "Analytical methods in electromagnetic nondestructive evaluation," Ph.D. Thesis, Stanford University, June 1984.

```
--     1   OF     2
-- 1 -  AD NUMBER: A171128
--48 -  SBI SITE HOLDING SYMBOL:       ATLF
-- 2 -  FIELDS AND GROUPS: 14/2, 9/3, 6/4
-  3 -  ENTRY CLASSIFICATION:   UNCLASSIFIED
-- 5 -  CORPORATE AUTHOR: SRI INTERNATIONAL  MENLO PARK CA
-- 6 -  UNCLASSIFIED TITLE:     ELECTROMAGNETIC SENSOR ARRAYS FOR
--       NONDESTRUCTIVE EVALUATION AND ROBOT CONTROL.
-  8 -  TITLE CLASSIFICATION:   UNCLASSIFIED
-- 9 -  DESCRIPTIVE NOTE: ANNUAL TECHNICAL REPT. NO.1, 1 SEP 84-31 AUG 85,
--10 -  PERSONAL AUTHORS: BAHR,A. J. ;ROSENGREEN,A. ;
--11 -  REPORT DATE:       OCT 31, 1985
- 12 -  PAGINATION:      28P
--15 -  CONTRACT NUMBER:  F49620-84-K-0011
--16 -  PROJECT NUMBER:   2306
--17 -  TASK NUMBER:      A2
- 18 -  MONITOR ACRONYM:  AFOSR
--19 -  MONITOR SERIES:   TR-86-0511
--20 -  REPORT CLASSIFICATION:  UNCLASSIFIED
--23 -  DESCRIPTORS:      *PROBES(ELECTROMAGNETIC), *DETECTORS, AUTOMATION,
-       ROBOTICS, NONDESTRUCTIVE TESTING, TEST EQUIPMENT, EXPERIMENTAL
--      DESIGN, THIN FILMS, MAGNETIC HEADS, MAGNETORESISTANCE
-          <<P FOR NEXT PAGE>> OR <<ENTER NEXT COMMAND>>
                                          «*MSG RECEIVED*  »
 ROW:24 COL:01                        DTIC/DROLS
```

END

1-87

DTIC